Energy Conversion and Management 88 (2014) 120–128

Contents lists available at ScienceDirect

Energy Conversion and Management

journal homepage: www.elsevier.com/locate/enconman

Investigation of bluff-body micro-flameless combustion

Seyed Ehsan Hosseini *, Mazlan Abdul Wahid

High-Speed Reacting Flow Laboratory, Faculty of Mechanical Engineering, Universiti Teknologi Malaysia, 81310 UTM Skudai, Johor, Malaysia

ARTICLE INFO

Article history:
Received 4 May 2014
Accepted 9 August 2014
Available online 7 September 2014

Keywords:
Micro-flameless combustion
Premixed
Methane
Bluff body

ABSTRACT

Characteristics of lean premixed conventional micro-combustion and lean non-premixed flameless regime of methane/air are investigated in this paper by solving three-dimensional governing equations. At moderate equivalence ratio ($\varnothing = 0.5$), standard k–ε and the eddy-dissipation concept are employed to simulate temperature distribution and combustion stability of these models. The effect of bluff-body on the temperature distribution of both conventional and flameless mode is developed. The results show that in the premixed conventional micro-combustion the stability of the flame is increased when a triangular bluff-body is applied. Moreover, micro-flameless combustion is more stable when bluff-body is used. Micro-flameless mode with bluff-body and 7% O_2 concentration (when N_2 is used as diluent) illustrated better performance than other cases. The maximum temperature in premixed conventional micro-combustion and micro-flameless combustion was recorded 2200 K and 1520 K respectively. Indeed, the flue gas temperature of conventional mode and flameless combustion was 1300 K and 1500 K respectively. The fluctuation of temperature in the conventional micro-combustor wall has negative effects on the combustor and reduces the lifetime of micro-combustor. However, in the micro-flameless mode, the wall temperature is moderate and uniform. The rate of fuel–oxidizer consumption in micro-flameless mode takes longer time and the period of cylinders recharging is prolonged.

1. Introduction

1.1. Development of micro-scale combustion

Recently, the demand for lightweight and compact energy resources has significantly increased because high energy density could not be supplied by traditional batteries. The demand for compact energy is expected to be increased due to development of electronic devices and thus micro-power will be required to supply energy of these enhanced functionalities [1,2]. Since the energy density (per unit mass or unit volume) of hydrocarbon fuels is much greater than the traditional batteries, micro-power generation based on combustion of hydrocarbons has been more considered. Furthermore, the negative impacts of conventional batteries on the environment upon disposal highlight the necessity of emergence of new micro-power generation methods for micro-electro-mechanic-systems (MEMS) [3]. Although, the package of combustion based micro-power generation could be significantly shrank, the demanded power is not compromised if the chemical energy of the fuel is utilized efficiently. Despite the low efficiency of micro-combustion systems, the priorities of combustion based micro-power generating in a few Watts within an extremely small volume was noticed [4]. In order to address the raising demand for small-scale electricity sources, various micro-combustion-based power generators have been developed. Hence, enhancement of flame stability and thermal efficiency of micro-combustors has become new challenge in combustion investigations [5,6]. The fundamental concepts of combustion characteristics of micro-scale combustors play crucial role in the improvement of system efficiency and optimization of the design. Since combustor volume is reduced in micro-scale combustion, conspicuous radical destruction and heat loss from micro-combustor walls are expected. Accordingly, application of micro-thermophotovoltaic (TPV) power generation in MEMS has been enhanced. Elimination of moving parts, high reliability and highly robust of TPV are the main characteristics of TPV which makes it suitable for application in commercial electronic devices [7]. In the recent years, conspicuous progress has been obtained in micro-scale combustion experimentally and numerically. These investigations have helped to understand the fundamentals of micro-combustion in terms of flammability limits, flame stability, emitter and thermal efficiency. Application of micro-combustion systems in MEMS was successfully experimented by Waitz et al. [8] in micro-turbines and Yang et al. [9] in the TPV in the last decade. Since the ratio of surface to the volume of micro-combustor is higher than regular combustors, the possibility of thermal quenching in micro-combustors is very high

* Corresponding author.
E-mail address: seyed.ehsan.hosseini@gmail.com (S.E. Hosseini).

http://dx.doi.org/10.1016/j.enconman.2014.08.023
0196-8904/

Nomenclature

μ_t	turbulent viscosity
P_k	turbulence kinetic energy production
P_b	effect of buoyancy
Y_M	the contribution of the fluctuating dilatation to the overall dissipation rate
$T_{s,o}$	outer surface temperature
T_∞	ambient temperature set at 300 K
h	natural convection coefficient considered constant value 5 W/m^2 K
σ	Stefan–Boltzmann constant (= 5.67 · 10^{-8} W/m^2 K^4)
ε	solid surface emissivity
C_ξ	volume fraction constant (= 2.1377)
v	kinematic viscosity
C_τ	time scale constant (= 0.4082)
σ_k	turbulent Prandtl numbers for k
σ_ε	turbulent Prandtl numbers
S_k, S_ε	user-defined source terms
$C_{1\varepsilon}$, $C_{2\varepsilon}$, $C_{3\varepsilon}$	constants
G_k	the generation of turbulence kinetic energy due to the mean velocity gradients
G_b	the generation of turbulence kinetic energy due to buoyancy
$\vec{J}_j$	diffusion flux of species j
k_{eff}	effective conductivity
Y_M	the contribution of the fluctuating dilatation in compressible turbulence to the overall dissipation rate

due to the extremely high heat loss from flame [10]. Therefore, stability of the flame in combustors with sub-millimeter size has become a new challenge [11]. Indeed, the stability of the flame in micro-scale combustors is influenced by absorption and destruction of generated combustion radicals [12]. Hence, feasibility of using catalyzed combustion [13] as well as application of external heat [14] and heat recirculation [15] were experimented. It was found that flame stability in micro-scale combustors depends strangely on the heat recirculation through combustor walls [16]. Preheating the reactants via heat transfer from high temperature region broads the reaction zone in micro-scale combustion [17]. To decrease heat loss to the ambient and impalement heat recirculation to the unburned zone, specific material should be selected. Therefore, material selection in micro-scale combustors is vital due to strong thermal coupling between reacting mixture and micro-combustor walls. Maruta et al. [18] pointed out that flame instabilities in non-premixed micro-scale combustion could be attributed to the interaction between flame structure and flame flow, heat loss and mass transfer limitations. Flame stability and characteristics of non-premixed sub-millimeter combustor was investigated by Prakash et al. [19]. The source of flame instabilities in premixed combustion of narrow channels was investigated by Sánchez-Sanz et al. [20]. Since the size of combustor shrinks to sub-millimeter in micro-scales, some combustion parameters such as flame ability, flame stability, flame thickness, heat loss, flow field and thermal efficiency are changed. Therefore, the role of numerical and computational investigation has been more highlighted in micro-combustion due to difficulty of measuring various quantities in such limited circumstance in experimental investigations. The impacts of various parameters such as combustor size, the geometry of combustor and boundary conditions on the flame temperature of hydrogen-air premixed micro-combustion were investigated by Li et al. [21] numerically. The authors stipulated that flame temperature in micro-scale combustion could be influenced by the mixture flow rate, the size and the geometry configuration of micro-combustor. Karagiannidis et al. [22] confirmed that a wide range of flammability could be offered in catalytic micro-combustors. The effects of equivalence ratio as well as inlet velocity on the structure of the premixed CH_4/air flame in micro-scale size were investigated by Feng et al. [23] computationally. It was found that the position of the flame is shifted to the downstream in high inlet velocities. Indeed, the highest flame temperature could be achieved in stoichiometric condition.

1.2. Flameless combustion technology

The commencement of flameless combustion research traced back to about 1990s, mainly attributed to the augmentation of the environmental concerns. Depletion of fossil fuel resources and anxieties about environmental issues conducted combustion research community to find environmentally friendly combustion technology and optimized fuel consumption [24]. Flameless combustion [25] or so-called moderate intensive low oxygen dilution (MILD) combustion [26] or high temperature air combustion technology (HITAC) [27] has been developed in the resent years because of its ability to combine high performance of combustion with extremely low pollutant formation [28]. The uniform temperature inside the chamber emerges perfectly stirred reactor circumstances. Since the peak of temperature reduces in flameless mode and hot spots are eliminated, NO_x formation reduces dramatically [29]. Indeed, low emission of flameless mode is attributed to the air dilution by inert gases such as CO_2 and N_2 [30,31]. In flameless combustion, the temperature of inlet diluted oxidizer is higher than self-ignition of the fuel, therefore ignition is eliminated [32]. Due to the significant potentials of the flameless mode to deal with various fuels, implementation of flameless combustion in micro-scale power generation could solve dilemma problems in micro-combustions and thus application of this model of combustion in micro-scale combustors could enhance combustion stability and thermal efficiency [33,34]. In the flameless mode, the reaction zone is distributed throughout the chamber consequently; the fluctuations of temperature are eliminated and uniform low temperature is observed. Furthermore, low oxygen concentration, elimination of audible and visible flame, low level of soot formation are the main characteristics of flameless mode [35]. Sine flameless mode shows complicated performance, analytical and computational investigation of this regime has received more attention especially in macro-scale combustors. Kim et al. [36] compared different reaction mechanisms in natural gas flameless combustion by using four different global reaction mechanisms and setting standard k–ε model and the eddy-dissipation concept (EDC). Dally [37] stipulated that based on the numerical results of centerline temperatures of the combustor achieved by adoption of k–ε and flamelet model, this settings are in good agreement with experimental results for CH_4 flameless combustion. Christo and Dally et al. [38] pointed out that it is necessary to consider differential diffusion effects in CFD modeling due to of calculations accuracy and the numerical results of eddy dissipation concept (EDC) solver shows higher accuracy. Hosseini and Wahid [39] investigated various aspects of biogas flameless combustion numerically. It was found that reaction time and Damköhler number plays crucial role in the computational settings. Although, characteristics of flameless combustion in macro-scale combustors have been developed numerically and experimentally, few documents could be found about micro-scale flameless mode. In the present paper, micro-flameless formation, temperature distribution in the

micro-flameless combustor, the effects of bluff-body on the performance of micro-flameless mode and the effects of diluent on the micro-flameless formation are investigated numerically and the results are compared to premixed micro-combustion.

2. Methodology

A three-dimensional (3D) micro-combustion is simulated by ANSYS 14 using ANSYS Modeler to design the micro-scale chamber and ANSYS Meshing to mesh the combustor [40]. In order to improve the convergence rate and scalar properties, mesh refinement is employed and therefore, grid resolution for smooth flow representation is ensured. In this investigation, a circular tube with 2 mm diameter is considered as a non-premixed micro-combustor. It is assumed that fuel jet is surrounded by the oxidizer, the diameter of inlet fuel is 1 mm and the length of micro-combustor is 15 mm. To simulate premixed conventional micro-combustor, a tube shape combustor with 2 mm diameter is considered where reactants are injected from the inlet step with 1 mm diameter because it was demonstrated that performance of conventional micro-combustion could be intensified by using inlet step [41]. Fig. 1 illustrates the schematic of studied micro-combustors and its unstructured mesh.

In this steady-state CFD simulation, methane (CH_4) is assumed as the fuel and the swirl velocity, pressure work and viscous forces are neglected. The equivalence ratio ($\varnothing$) of both premixed conventional combustion and non-premixed flameless mode is 0.5. Since the length of micro-combustor is longer than the molecular mean-free path of the reactants through the micro-combustor, reactants treat as continuums and thus Navier–Stokes equations are valid [42]. Pervious investigations indicated that the stability of turbulent micro-combustion is higher than laminar one [43,44]. In addition, enhancement of turbulence aids flameless regime to be sustained. Therefore, standard k–ε turbulence model with following transport equations is applied to model flameless micro-combustion system [39].

$$\frac{\partial}{\partial t}(\rho k)+\frac{\partial}{\partial x_i}(\rho k u_i)=\frac{\partial}{\partial x_j}\left[\left(\mu+\frac{\mu_t}{\sigma_k}\right)\frac{\partial k}{\partial x_j}\right]+P_k+P_b-\rho\varepsilon-Y_M+S_k \quad (1)$$

$$\frac{\partial}{\partial t}(\rho \varepsilon)+\frac{\partial}{\partial x_i}(\rho \varepsilon u_i)=\frac{\partial}{\partial x_j}\left[\left(\mu+\frac{\mu_t}{\sigma_\varepsilon}\right)\frac{\partial k}{\partial x_j}\right]+C_{1\varepsilon}\frac{\varepsilon}{k}(P_k+C_{3\varepsilon}P_b)-C_{2\varepsilon\rho}\frac{\varepsilon^2}{k}+S_\varepsilon \quad (2)$$

S_k, S_ε user-defined source terms, $C_{1\varepsilon}$, $C_{2\varepsilon}$, $C_{3\varepsilon}$ are constants. Where turbulent viscosity and turbulence kinetic energy production are modeled by Eqs. (3) and (4) respectively.

$$\mu_t=\rho C_\mu\frac{k^2}{\varepsilon} \quad (3)$$

$$P_k=-\rho\overline{u_i'u_j'}\frac{\partial u_j}{\partial u_i} \quad (4)$$

The accuracy and robustness of k–ε model for turbulent flows is very high. Thus, the accuracy of CFD modeling could be enhanced due to fully turbulent circumstance in flameless combustion chamber [45].

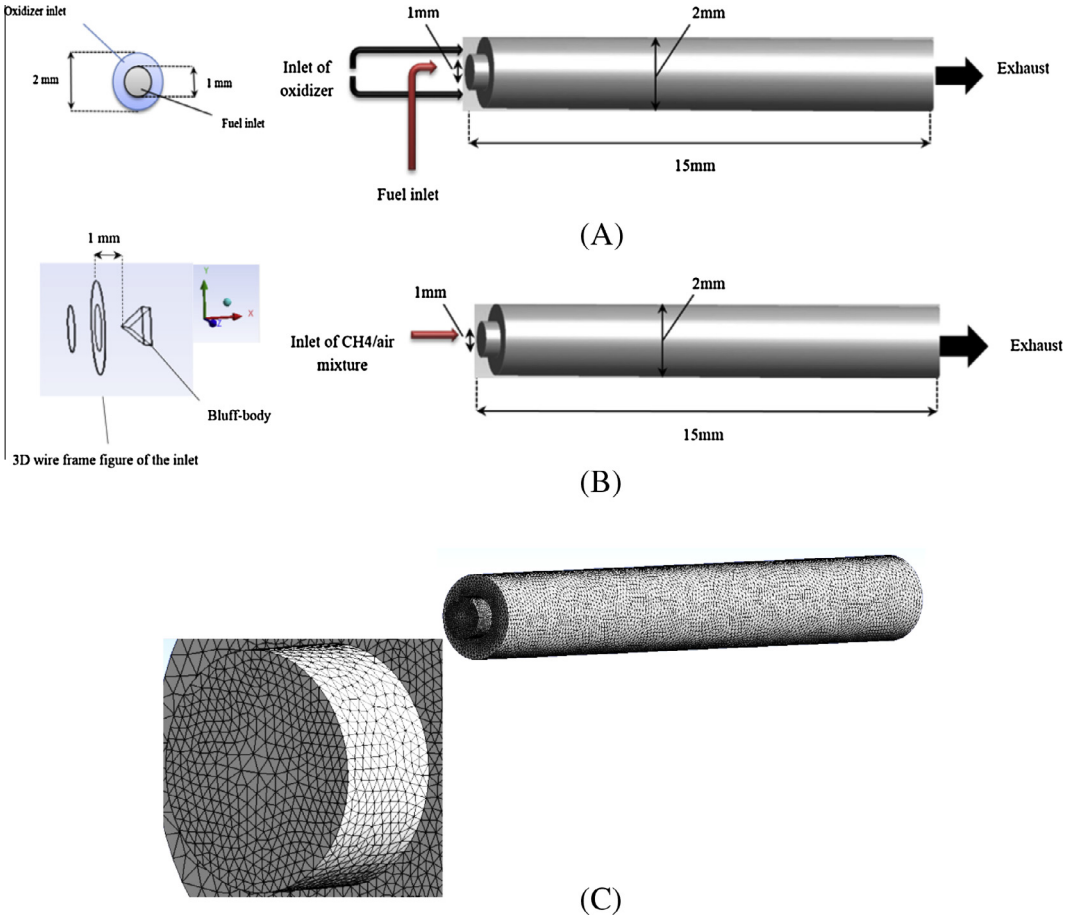

Fig. 1. The schematic of micro-combustor (A) non-premixed combustor, (B) premixed combustor and (C) unstructured mesh of the micro-combustor.

Eqs. (5) and (6) named Reynolds-average Navier–Stokes (RANS) equations are employed for continuity and momentum in turbulent condition.

$$\frac{\partial \rho}{\partial t}+\frac{\partial}{\partial x_i}(\rho u_i)=0 \tag{5}$$

$$\frac{\partial}{\partial t}(\rho u_i)+\frac{\partial}{\partial x_j}(\rho u_i u_j)=-\frac{\partial p}{\partial x_i}+\frac{\partial}{\partial x_j}\left[\mu\left(\frac{\partial u_i}{\partial x_j}+\frac{\partial u_j}{\partial x_i}-\frac{2}{3}\delta_{ij}\frac{\partial u_i}{\partial x_i}\right)\right]+\frac{\partial}{\partial x_j}(-\rho\overline{u_i' u_j'}) \tag{6}$$

The energy equation in turbulent circumstance developed by Ref [39] is applied in this case.

$$\frac{\partial}{\partial t}(\rho E)+\nabla\cdot\left(\vec{V}(\rho E+p)\right)=\nabla\cdot\left(k_{eff}\nabla T-\sum jh_j\vec{J}_j+(\bar{\tau}_{eff}\cdot\vec{V})\right)+S_h \tag{7}$$

where k_{eff} is effective conductivity, $\vec{J}_j$ is diffusion flux of species j, S_h is a combination of heat chemical reactant and every other heat resource which are defined.

On the right hand side of Eq. (7), the first three terms represent energy transfer due to conduction.

Second-order scheme is set to solve related governing equations. The residual of all variables is adopted 10^{-3} except energy which is set 10^{-6} to ensure the convergence of the solution. The swirl velocity is neglected in both conventional flame and flameless mode. Since no remarkable difference in terms of flame temperature was reported in fully developed and uniform inlet velocity of the mixture in the micro-combustor [21], the inlet velocity of mixture is considered uniform.

Methane-air-2step by following equations [46] is employed to model species transport.

$$CH_4+3/2O_2 \rightarrow CO+2H_2O \quad \Delta G=-632.68\ \text{kJ/mol} \tag{8}$$

$$CO+1/2O_2 \leftrightarrow CO_2 \quad \Delta G=-257.19\ \text{kJ/mol} \tag{9}$$

The variation of equilibrium constant against the temperature can be written as Eq. (10).

$$K=\frac{\prod_j (X_j)^{\upsilon_j}}{\prod_i (X_i)^{\upsilon_i}} \tag{10}$$

where X_i, X_j, υ_i and υ_j are the molar fractions of the reactant i, product j, the stoichiometric coefficients of the reactant i and product j respectively.

For computation of Arrhenius parameters of reaction (9) (as an example) the equilibrium constant K_1 and K_2 are defined as:

$$K_1=\frac{(X_{CO_2})^{\upsilon_{CO_2}}}{(X_{O_2})^{\upsilon_{O_2}}(X_{CO})^{\upsilon_{CO}}}=\frac{X^1_{CO_2}}{X^{0.5}_{O_2}X^1_{CO}} \tag{11}$$

$$K_2=\frac{X^{0.5}_{O_2}X^1_{CO}}{X^1_{CO_2}}=\frac{1}{K_1} \tag{12}$$

The backward rates and the forward rates are derived from equilibrium constants of reaction as shown in Eq. (13).

$$k_{b_i}=\frac{k_{f_i}}{K_i} \tag{13}$$

(b for backward and f for forward reaction).

Therefore,

$$k_{f_1}\left([O_2]^{1/2}[CO]^1-\frac{1}{K_1}[CO_2]^1\right)=k_{f_2}k_1\left([O_2]^{1/2}[CO]^1-\frac{1}{K_1}[CO_2]^1\right) \tag{14}$$

Reaction rate is calculated by Arrhenius equation [47].

$$k=AT^{\beta}e^{-\left(\frac{E}{RT}\right)} \tag{15}$$

where k is reaction rate, R is gas constant, A is pre-exponential, T is temperature and β is dimensionless number of order one.

Hence, Arrhenius parameters of reaction (9) is written as:

$$k_{f_2}=\frac{k_{f_1}}{K_1}=\frac{A_1\exp\left(\frac{-T_{a1}}{T}\right)}{K_1}=A_2\exp\left(\frac{-T_{a2}}{T}\right) \tag{16}$$

Viscosity, thermal conductivity and specific heat are calculated by considering the average of species mass fraction. Radiation heat transfer between micro-combustor walls is considered. Discrete ordinates (DO) model is used to simulate surface-to-surface radiation heat transfer. Indeed, non-slip internal walls are assumed and no species flux normal to the surfaces is considered. It is assumed that heat losses from micro-combustor surfaces to the ambient by radiation and convection heat transfer.

$$q=h(T_{S,O}-T_\infty)+\varepsilon\sigma(T^4_{S,O}-T^4_\infty) \tag{17}$$

Eddy dissipation concept (EDC) is used to model turbulence–chemistry interaction. EDC includes detail of chemical mechanisms in turbulent flows when reaction takes place in small turbulent conditions or so-called fine scales. The model of fine scales length fraction is modeled br Eq. (18) [48].

$$\xi^*=C_\xi\left(\frac{v\varepsilon}{k^2}\right)^{\frac{1}{4}} \tag{18}$$

where * denotes fine-scale quantities.

It is assumed that the combustion at fine scales occurs at constant pressure when the current species and temperature in the cell is taken the initial conditions. Indeed Arrhenius equation governs the speed of the reactions over the time scale presented in Eq. (19).

$$\tau^*=C_\tau\left(\frac{\upsilon}{\varepsilon}\right)^{\frac{1}{2}} \tag{19}$$

In most of the previous investigations about macro-scale flameless combustion technology, dilution of oxidizer has been mentioned as one of the fundamentals of flameless regime formation. It has been stipulated that when the percentage of oxygen in the combustion air increases up to 15%, flame is constituted [39]. The boundary conditions of this study have been selected based on the previous experiments in macro-scale flameless mode. In conventional combustion the temperature of oxidizer (consist of 21% O_2 and 79% N_2 by vol.) is set 300 K and in micro-flameless mode the temperature of inlet oxidizer (case1: 5% O_2 and 95% N_2, case2: 7% O_2 and 93% N_2 by vol.) is adopted 900 K, higher than self-ignition temperature of methane.

In the inlet of the micro-flameless combustor, it is assumed that $u = cte$, $T = cte$ and $\frac{\partial v}{\partial y}=\frac{\partial w}{\partial z}=0$.

Indeed, in the exhaust $\frac{\partial u}{\partial x}=\frac{\partial v}{\partial y}=\frac{\partial w}{\partial z}=0$ and $\frac{\partial P}{\partial x}=\frac{\partial P}{\partial y}=\frac{\partial P}{\partial z}=0$. A summary of the boundary conditions of the simulation is presented in Table 1.

3. Results and discussion

The grid independent test is done by changing the number of elements to the finer elements. The number of meshes were set 206,190, 254,202 and 312,021 respectively to observe the changes of the results. However, meaningful variations were not observed in the recorded results therefore the numerical computation is done with 40,073 nodes and 206,190 elements to reduce the number of iterations. The validation of the numerical records of micro-combustion in conventional mode was done by comparing the

Table 1
Boundry condition of simulation.

Properties	Premixed conventional micro-combustion	Micro-flameless combustion
Velocity	Uniform $V_{inlet\ mixture}$ = 10 m/s	Uniform $V_{inlet\ oxidizer}$ = 30 m/s $V_{inlet\ CH4}$ = 1.32 m/s
Temperature	Uniform $T_{inlet\ mixture}$ = 300 K	Uniform $T_{inlet\ oxidizer}$ = 900 K $T_{inlet\ CH4}$ = 300 K
Oxidizer ingredients	–	N_2: 93–95% O_2: 5–7%
Density of oxidizer (kg/m^3)	–	0.382–0.383
Density of mixture/fuel (kg/m^3)	1.238	0.770
Pressure gage	0 Pa	0 Pa
Wall material	Steel	Steel
Wall slip	Non-slip	Non-slip
Thermal conduction	Mixed (convection + radiation)	Mixed (convection + radiation)

results with previous experimental [49] and numerical [21] results. Fig. 2 compares the axial and radial temperature profile of simulated micro-flameless mode with respect to various numbers of meshes.

3.1. Premixed and non-premixed conventional micro-combustion

Most of previous investigations about conventional micro-combustion were done in premixed circumstances where fuel and oxidizer were well stirred before injection to the micro-combustor. Due to the small length and diameter of micro-combustor, application of premixed combustion method could be the best strategy to optimize the efficiency of the combustor. Moreover, the stability of the flame and efficiency of micro-combustor could be enhanced by using bluff-body [43]. In this regard, a triangular bluff-body is designed at the inlet of the micro-combustor to notice the effect of bluff-body. Depicts temperature distribution inside the micro-combustor in premixed and non-premixed conventional combustion.

Based on the concept of chemical kinetics, chemical reaction time reduces when the reaction rate increases. In the micro-combustors, higher reaction temperature ensures reduction of reaction time. Hence, enhancement of flame temperature as well as heat loss mitigation from the micro-combustor could ensure the flame stability [50]. From Fig. 3, it can be construed that making stable flame in the non-premixed conventional micro-combustion is not as convenience as premixed combustion even when bluff-body is employed. In the other hand, in premixed conventional micro-combustion flame is constituted in the downstream region of the combustor and it makes some limitation for inlet velocity of the mixture, thus it is preferred to apply premixed combustion with bluff-body in conventional combustion of micro-scales.

3.2. Micro-flameless combustion

As it was mentioned, in flameless regime high temperature diluted oxidizer injected to the furnace, hence for flameless combustion mode non-premixed regime is utilized. In order to enhance the stability of flameless mode, a bluff-body is used in the inlet of the micro combustor. Fig. 4 displays the structure of flameless micro-combustion in various cases. Indeed, temperature distribution along the centerline and wall temperature of different conditions of micro-flameless mode has been demonstrated.

Micro-flameless combustion is demonstrated better performance in terms of flameless stability and temperature distribution when bluff-body is applied at the inlet of combustor. Fig. 4(A) and (B) illustrate that the peak of temperature shifted to the inlet of the micro-flameless combustor (5% and 7% oxygen concentration) when the bluff-body was employed. The maximum temperature

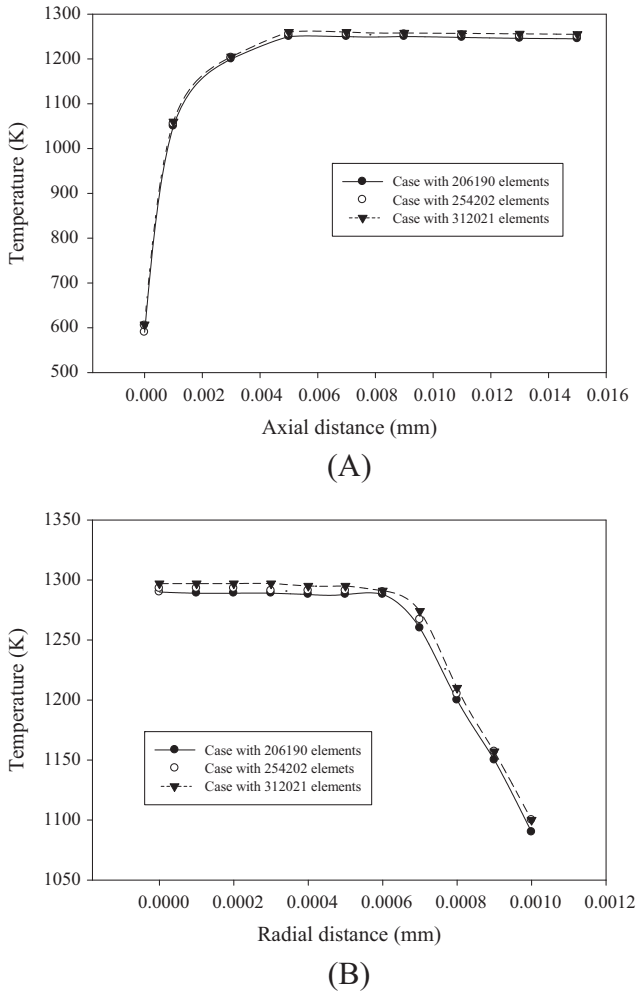

Fig. 2. (A) Axial and (B) radial temperature profile of simulation (at X = 0.0075 mm from the inlet).

in bluff-body micro-flameless combustion of CH_4 was recorded 1551 K and 1376 K when oxygen concentration in the oxidizer was 7% and 5% by volume respectively.

From previous studies, it was found that both CO_2 and N_2 are eligible to be applied as diluent to dilute the oxidizer in flameless mode [51]. In order to evaluate the performance of micro-flameless mode in different conditions, two various cases were solved (case one: O_2 concentration is 7% and N_2 is applied as diluent, case two:

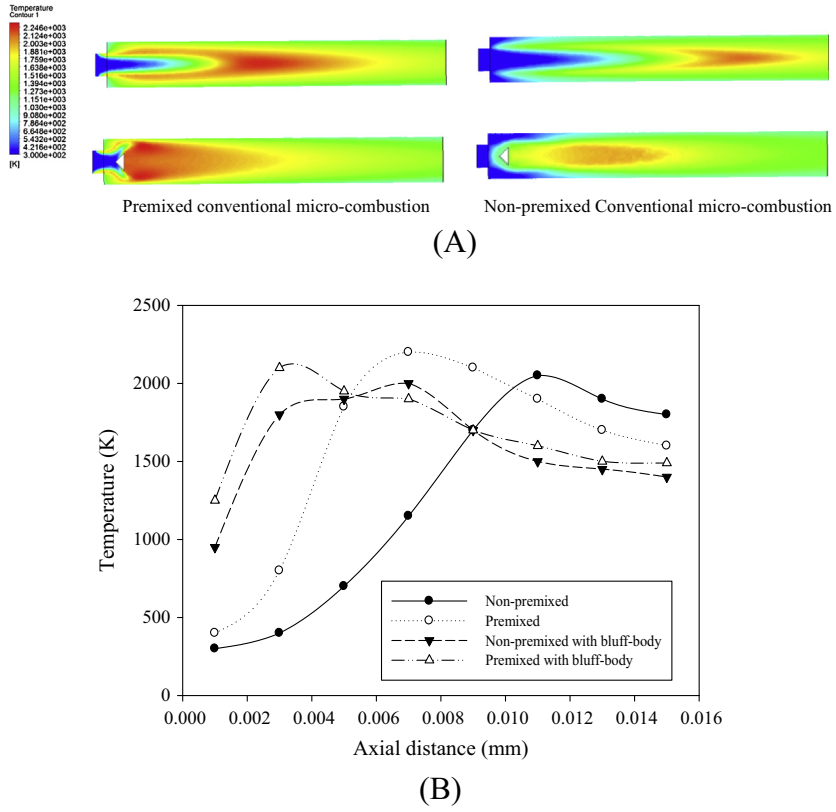

Fig. 3. (A) Flame structure in premixed and non-premixed conventional micro-combustion with and without bluff-body and (B) temperature distribution along centerline of the chamber.

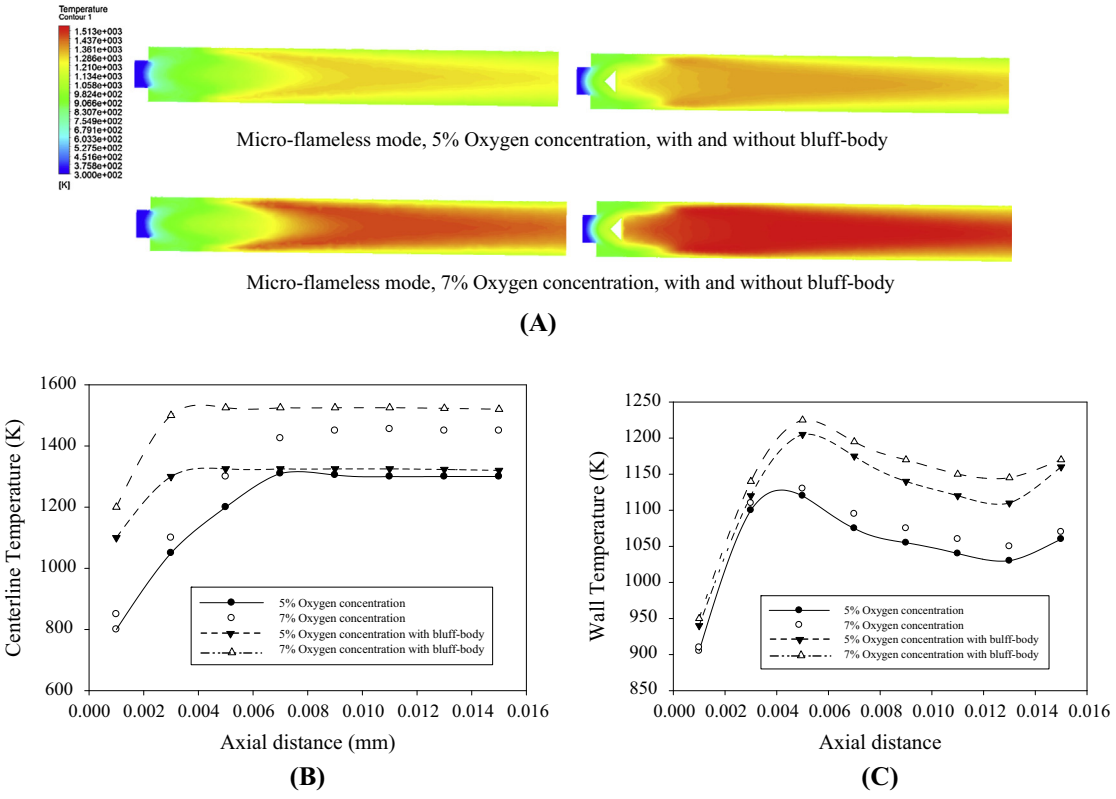

Fig. 4. (A) Temperature contour of micro-flameless combustion, (B) temperature distribution along the centerline and (C) wall temperature of the micro-flameless mode.

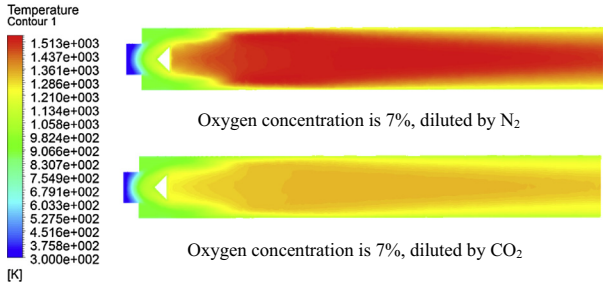

Fig. 5. The effects of various diluent on the temperature distribution with in the micro-flameless mode.

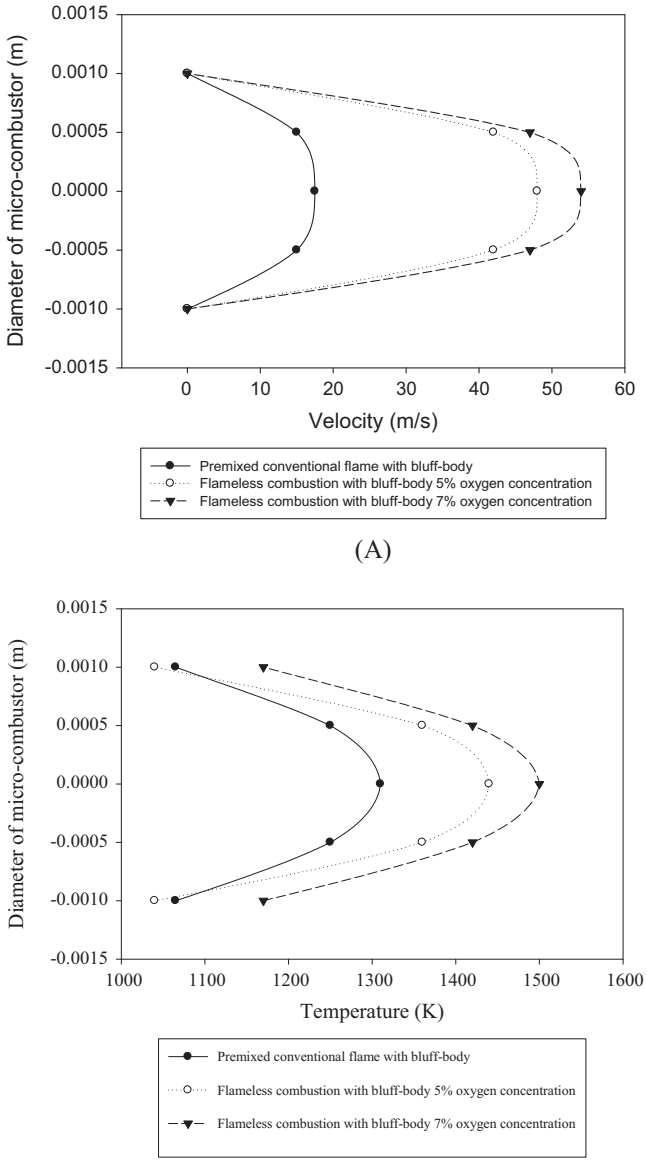

Fig. 6. (A) The outlet velocity profile and (B) the outlet temperature profile.

O_2 concentration is 7% and CO_2 is applied as diluent). The maximum temperature of combustor was recorded 1551 K and 1345 K when N_2 and CO_2 were applied as diluent respectively. Therefore, when N_2 is applied as diluent, micro-flameless system shows better performance in terms of achieving higher temperatures. The lower

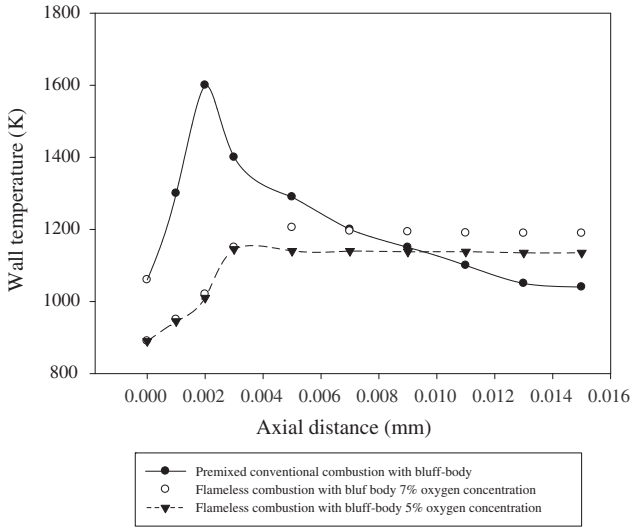

Fig. 7. Wall temperature.

temperature in case two could be attributed to the high radiation heat transfer via CO_2 particles in the micro-combustor. Fig. 5 illustrates the effects of various diluent on the temperature distribution with in the micro-flameless mode.

In order to interpret the micro-combustion phenomena in both conventional and flameless mode, Damköhler (D_a) number should be taken into account. The interaction between mixing (or flow time scale) and reaction in a combustion system is represented by D_a number [39].

$$D_a = \tau_f / \tau_c \tag{20}$$

where τ_f is flow time-scale and τ_c is chemical time-scale.

Large D_a numbers occurs in mixing controlled flames and it depicts that reactants and products are quickly stirred in a high turbulence circumstance. In contrast, low D_a numbers demonstrates slow chemical reactions [52]. Based on the calculations, both reaction rates (R_1 from Eq. (8) and R_2 from Eq. (9)) in the micro-flameless combustion mode with 7% O_2 concentration ($R_1 = 0.7433$, $R_2 = 0.7195$) is higher than conventional micro-combustion ($R_1 = 0.6915$, $R_2 = 0.6335$). In addition, D_a number is much greater in micro-flameless regime and thus, complete and stabile energy conversion is expected in micro-flameless combustion mode.

In conventional premixed micro-combustion, when the mixture inlet flow rate increases, the flame length becomes longer and the flame is formed further downstream of the inlet of the combustor. Therefore, longer heating length is needed for high flow rate mixtures to be heated up and reach ignition temperature. Hence, the velocity of the mixture is one of the limitations of conventional micro-combustors. Since ignition is eliminated in flameless mode and visible flame is not constituted, higher velocities could be adopted in micro-flameless mode, which could be ideal condition for micro-turbines. Furthermore, the temperature of flue gases influences significantly on the efficiency of gas turbine. It means that high exhaust gas temperatures could enhance the efficiency of the micro-turbine [53]. Fig. 6 demonstrates the outlet velocity and temperature profile of micro-flameless regime in the various cases.

Based on Fig. 7, the results show that the outlet velocity as well as outlet temperature of exhaust gases of micro-flameless combustion (7% oxygen concentration) is significantly higher than micro-flameless mode with 5% oxygen concentration and conventional

micro-combustion. In Fig. 3 it was shown that the maximum temperature of conventional premixed micro-combustion is around 2200 K, which depicts flame temperature. However, from Fig. 6B outlet temperature of exhaust gases is around 1300 K. In contrast, maximum temperature and outlet temperature of flue gases in flameless mode are recorded 1520 K and 1500 K respectively. It means, temperature inside the micro-combustor is more homogeneous in flameless mode and hot spots are eliminated. Therefore, the body of micro-combustor could be protected from elevated temperatures. Fig. 7 shows the wall temperature in conventional and flameless mode. The fluctuation of wall temperature in conventional mode ruins the material of the combustor wall. Indeed, these fluctuations have negative effects on the emitter efficiency of the micro-combustor in micro-TPV application.

The other important characteristic of micro-flameless mode is its low fuel and oxidizer consumption. Since micro-combustors are usually applied in the sensitive situations, it is vital to decrease the size of fuel and oxidizer cylinders and increase the period of their recharge simultaneously. The rate of CH_4-oxidizer consumption in premixed conventional micro-combustion and non-premixed micro-flameless was recorded 2.77×10^{-3} g/s–2.63×10^{-2} g/s and 8.05×10^{-4} g/s–2.7×10^{-2} g/s respectively. It means that with respect to the specific energy generation, consumption of a specific volume of CH_4-oxidizer in micro-flameless takes longer time and the period of cylinder recharging is prolonged.

4. Conclusion

The characteristics of micro-flameless combustion was investigated by 3D simulation. The effect of bluff-body on the temperature distribution and blow-off limit of micro-flameless mode was simulated. The results confirm that the stability of the premixed conventional micro-flame increases when a triangular bluff-body is applied. Indeed, combustion is more stable in micro-flameless mode when bluff-body is used. Micro-flameless combustion with bluff-body and 7% O_2 concentration showed better performance (in terms of higher peak of temperature and higher flue gases velocity) than other cases in the flameless modes. Moreover, when N_2 is used as diluent, the maximum temperature of micro-flameless mode increases compared to CO_2 utilization. It was demonstrated that the peak temperature of premixed conventional micro-combustion (around 2200 K) is much higher than the maximum temperature of micro-flameless combustion (around 1520 K). However, the temperature of exhaust gases (which plays crucial role on the performance of the micro-turbines) in conventional mode (1300 K) is lower than micro-flameless regime (1500 K). The fluctuations of temperature in the conventional combustor wall could damage the inner wall of the micro-combustor, but in the flameless mode, the wall temperature is moderate and uniform. Furthermore, these fluctuations have negative effects on the emitter efficiency the performance of micro-TPV could be reduced. With respect to the specific energy generation, the rate of CH_4/oxidizer consumption in micro-flameless mode is lower than conventional combustion. Some advantages of micro-flameless combustion could be summarized as below:

- In the micro-flameless system, combustion stability and temperature uniformity inside the micro-combustor increase compared to the conventional mode.
- Reduction of fuel and oxidizer consumption could be obtained in micro-flameless mode, thus the combustion system package is more compact.
- The flame quenching which has been mentioned as one of the most important limitations of the conventional micro-combustion could be eliminated in the micro-flameless mode.
- Due to lift-off of the flame, the inlet velocity of the mixture is limited in the conventional micro-combustion, which could be a weak point in the micro-turbine systems. However, in the micro-flameless, higher inlet velocities could be achieved due to the elimination of the flame.
- In micro-flameless combustion, inside temperature of the combustor is lower than conventional mode. Hence, a broader range of materials could be employed in a micro-flameless system.

References

[1] Chou SK, Yang WM, Chua KJ, Li J, Zhang KL. Development of micro power generators – a review. Appl Energy 2011;88:1–16.
[2] Yang W, Chou S, Shu C, Xue H, Li Z, Li D, et al. Microscale combustion research for application to micro thermophotovoltaic systems. Energy Convers Manage 2003;44:2625–34.
[3] Yang WM, Chua KJ, Pan JF, Jiang DY, An H. Development of micro-thermophotovoltaic power generator with heat recuperation. Energy Convers Manage 2014;78:81–7.
[4] Fernandez-Pello AC. Micropower generation using combustion: issues and approaches. Proc Combust Inst 2002;29:883–99.
[5] Zhou J, Wang Y, Yang W, Liu J, Wang Z, Cen K. Improvement of micro-combustion stability through electrical heating. Appl Therm Eng 2009;29:2373–8.
[6] Sahota GPS, Khandelwal B, Kumar S. Experimental investigations on a new active swirl based microcombustor for an integrated micro-reformer system. Energy Convers Manage 2011;52:3206–13.
[7] Colangelo G, de Risi A, Laforgia D. Experimental study of a burner with high temperature heat recovery system for TPV applications. Energy Convers Manage 2006;47:1192–206.
[8] Waitz IA, Gauba G, Tzeng Y-S. Combustors for micro-gas turbine engines. J Fluids Eng 1998;120:109.
[9] Yang WM, Chou SK, Shu C, Li ZW, Xue H. Development of microthermophotovoltaic system. Appl Phys Lett 2002;81:5255.
[10] Norton DG, Vlachos DG. A CFD study of propane/air microflame stability. Combust Flame 2004;138:97–107.
[11] Aghalayam P, Vlachos DG. Roles of thermal and radical quenching in emissions of wall-stabilized hydrogen flames. AIChE J 1998;44:2025–34.
[12] Kim K, Lee D, Kwon S. Effects of thermal and chemical surface–flame interaction on flame quenching. Combust Flame 2006;146:19–28.
[13] Boyarko GA, Sung C-J, Schneider SJ. Catalyzed combustion of hydrogen–oxygen in platinum tubes for micro-propulsion applications. Proc Combust Inst 2005;30:2481–8.
[14] Fan A, Minaev S, Kumar S, Liu W, Maruta K. Regime diagrams and characteristics of flame patterns in radial microchannels with temperature gradients. Combust Flame 2008;153:479–89.
[15] Taywade UW, Deshpande AA, Kumar S. Thermal performance of a micro combustor with heat recirculation. Fuel Process Technol 2013;109:179–88.
[16] Ronney P. Analysis of non-adiabatic heat-recirculating combustors. Combust Flame 2003;135:421–39.
[17] Leach TT, Cadou CP, Jackson GS. Effect of structural conduction and heat loss on combustion in micro-channels. Combust Theory Model 2006;10:85–103.
[18] Maruta K, Kataoka T, Kim NI, Minaev S, Fursenko R. Characteristics of combustion in a narrow channel with a temperature gradient. Proc Combust Inst 2005;30:2429–36.
[19] Prakash S, Armijo AD, Masel RI, Shannon MA. Flame dynamics and structure within sub-millimeter combustors. AIChE J 2007;53:1568–77.
[20] Sánchez-Sanz M. Premixed flame extinction in narrow channels with and without heat recirculation. Combust Flame 2012;159:3158–67.
[21] Li J, Chou SK, Yang WM, Li ZW. A numerical study on premixed micro-combustion of CH_4–air mixture: effects of combustor size, geometry and boundary conditions on flame temperature. Chem Eng J 2009;150:213–22.
[22] Karagiannidis S, Mantzaras J, Jackson G, Boulouchos K. Hetero-/homogeneous combustion and stability maps in methane-fueled catalytic microreactors. Proc Combust Inst 2007;31:3309–17.
[23] Feng L, Liu Z, Li Y. Numerical study of methane and air combustion inside a small tube with an axial temperature gradient at the wall. Appl Therm Eng 2010;30:2804–7.
[24] Hosseini SE, Wahid MA. Biogas utilization: experimental investigation on biogas flameless combustion in lab-scale furnace. Energy Convers Manage 2013;74:426–32.
[25] Wünning JA, Wünning JG. Flameless oxidation to reduce thermal no-formation. Prog Energy Combust Sci 1997;23:81–94.
[26] Weber R, Smart J. On the (MILD) combustion of gaseous, liquid, and solid fuels in high temperature preheated air. Proc Combust Inst 2005;30(2):2623–9.
[27] Gupta A. Thermal characteristics of gaseous fuel flames using high temperature air. Eng Gas Turbines Power 2004;126(1):9–19.
[28] Hosseini SE, Wahid MA, Abuelnuor AAA. Biogas flameless combustion: a review. Appl Mech Mater 2013;388:273–9.
[29] Hosseini SE, Wahid MA, Abuelnuor AAA. High temperature air combustion: sustainable technology to low NO_x formation. Int Rev Mech Eng 2012;6:947–53.

[30] Hosseini SE, Salehirad S, Wahid MA, Sies MM, Saat A. Effect of diluted and preheated oxidizer on the emission of methane flameless combustion. 4TH Int Meet Adv THERMOFLUIDS (IMAT 2011), vol. 1440. AIP Publishing; 2012, p. 1309–12.
[31] Choi G-M, Katsuki M. Advanced low NO_x combustion using highly preheated air. Energy Convers Manage 2001;42:639–52.
[32] Hosseini SE, Wahid MA, Abuelnuor AAA. Pollutant reduction and energy saving in industrial sectors by applying high temperature air combustion method. Int Rev Mech Eng 2012;6:1667–72.
[33] Ju Y, Maruta K. Microscale combustion: technology development and fundamental research. Prog Energy Combust Sci 2011;37:669–715.
[34] Parente A, Galletti C, Riccardi J, Schiavetti M, Tognotti L. Experimental and numerical investigation of a micro-CHP flameless unit. Appl Energy 2012;89:203–14.
[35] Rebola A, Coelho PJ, Costa M. Assessment of the performance of several turbulence and combustion models in the numerical simulation of a flameless combustor. Combust Sci Technol 2013;185:600–26.
[36] Kim JP, Schnell U, Scheffknecht G. Comparison of different global reaction mechanisms for MILD combustion of natural gas. Combust Sci Technol 2008;180:565–92.
[37] Dally B. Effect of fuel mixture on moderate and intense low oxygen dilution combustion. Combust Flame 2004;137:418–31.
[38] Christo FC, Dally BB. Modeling turbulent reacting jets issuing into a hot and diluted coflow. Combust Flame 2005;142:117–29.
[39] Hosseini SE, Bagheri G, Wahid MA. Numerical investigation of biogas flameless combustion. Energy Convers Manage 2014;81:41–50.
[40] Fluent A. 12.0 Theory Guide. Ansys Inc.; 2009.
[41] Yang W, Chou S, Shu C, Li Z, Xue H. Combustion in micro-cylindrical combustors with and without a backward facing step. Appl Therm Eng 2002;22:1777–87.
[42] Wan J, Yang W, Fan A, Liu Y, Yao H, Liu W, et al. A numerical investigation on combustion characteristics of H_2/air mixture in a micro-combustor with wall cavities. Int J Hydrogen Energy 2014:1–9.
[43] Fan A, Wan J, Liu Y, Pi B, Yao H, Liu W. Effect of bluff body shape on the blow-off limit of hydrogen/air flame in a planar micro-combustor. Appl Therm Eng 2014;62:13–9.
[44] Kuo CH, Ronney PD. Numerical modeling of non-adiabatic heat-recirculating combustors. Proc Combust Inst 2007;31:3277–84.
[45] Wilcox D. Turbulence modeling for CFD; 1998.
[46] Westbrook CK, Dryer FL. Simplified reaction mechanisms for the oxidation of hydrocarbon fuels in flames. Combust Sci Technol 1981;27:31–43.
[47] Tien JH, Stalker RJ. Release of chemical energy by combustion in a supersonic mixing layer of hydrogen and air. Combust Flame 2002;131:329–48.
[48] Ansys A. 14.0 Theory Guide. Fluent, Ansys, 140 Theory Guid Ansys Inc. 5 n.d.
[49] Li J, Chou SK, Huang G, Yang WM, Li ZW. Study on premixed combustion in cylindrical micro combustors: transient flame behavior and wall heat flux. Exp Therm Fluid Sci 2009;33:764–73.
[50] Bagheri G, Hosseini SE, Wahid MA. Effects of bluff body shape on the flame stability in premixed micro-combustion of hydrogen–air mixture. Appl Therm Eng 2014;67:266–72.
[51] Tsuji H, Gupta AK, Hasegawa T, Katsuki M, Kishimoto K, Morita M. High temperature air combustion: from energy conservation to pollution reduction (Google eBook). CRC Press; 2002.
[52] Isaac BJ, Parente A, Galletti C, Thornock JN, Smith PJ, Tognotti L. A novel methodology for chemical time scale evaluation with detailed chemical reaction kinetics. Energy Fuels 2013;27:2255–65.
[53] Cao HL, Xu JL. Thermal performance of a micro-combustor for micro-gas turbine system. Energy Convers Manage 2007;48:1569–78.